IOPscience iopscience.iop.org

Home Search Collections Journals About Contact us My IOPscience

Anomalous bias dependence in magnetic tunnel junctions based on half-metallic CrO_2 with heteroepitaxial SnO_2 tunnel barrier

This article has been downloaded from IOPscience. Please scroll down to see the full text article.

2009 EPL 87 47006

(http://iopscience.iop.org/0295-5075/87/4/47006)

View the table of contents for this issue, or go to the journal homepage for more

Download details:
IP Address: 138.16.58.229
The article was downloaded on 12/07/2010 at 18:34

Please note that terms and conditions apply.

epl — A Letters Journal Exploring the Frontiers of Physics

August 2009

EPL, **87** (2009) 47006
doi: 10.1209/0295-5075/87/47006

www.epljournal.org

Anomalous bias dependence in magnetic tunnel junctions based on half-metallic CrO_2 with heteroepitaxial SnO_2 tunnel barrier

Guo-Xing Miao[1,2(a)], Gang Xiao[2] and Arunava Gupta[1]

[1] *MINT center, University of Alabama - Tuscaloosa, AL 35487, USA*
[2] *Physics Department, Brown University - Providence, RI 02912, USA*

received 29 June 2009; accepted in final form 5 August 2009
published online 7 September 2009

PACS 73.40.Gk – Tunneling
PACS 72.25.-b – Spin polarized transport
PACS 73.40.Sx – Metal-semiconductor-metal structures

Abstract – We report on the anomalous bias dependence of tunneling magnetoresistance (TMR) in ($CrO_2/SnO_2/Co$)-based magnetic tunnel junctions as a function of barrier thickness. For a relatively thin SnO_2 barrier, the TMR is asymmetric and exhibits sign reversal at a specific bias voltage with varying thickness due to defect mediated resonant tunneling. On the other hand, diffusive transport dominates for sufficiently thick SnO_2 barriers, and a diverging TMR is observed close to zero bias.

Copyright © EPLA, 2009

Magnetic tunneling junctions (MTJs) are under intensive investigation for a variety of applications, including magnetic storage and memory devices. Switching the relative orientation of the two ferromagnetic electrodes in the MTJ from parallel (P) to antiparallel (AP) alignment alters the available tunneling density of states, with the resultant resistance change of the junction termed as tunneling magnetoresistance (TMR). A model for spin-polarized tunneling had been first proposed by Jullière in 1975 [1]. According to this simple model, a straightforward approach to enhance TMR is to use an electrode material with high spin polarization, in particular half-metallic ferromagnets for which the polarization value approaches 100%. CrO_2 is a known half-metal with the highest experimentally measured spin polarization at low temperatures [2]. Consequently, rutile-based heterostructures based on half-metallic CrO_2, such as $CrO_2/TiO_2/CrO_2$ and $CrO_2/RuO_2/CrO_2$, have been proposed as potentially excellent candidates for spintronic device applications [3,4]. CrO_2 is a metastable phase, and its surface tends to be easily reduced under normal atmospheric conditions to form the more stable Cr_2O_3 phase, which is an antiferromagnetic insulator with a Néel temperature of 307 K. Therefore a tunnel junction can be readily fabricated by directly depositing a ferromagnetic Co thin-film electrode on top of CrO_2, with the Cr_2O_3 surface layer serving as a natural barrier [5]. An inverse TMR of −8% has been observed in CrO_2/Co MTJs at 5 K [5]. Inverse TMR corresponds to a negative sign of the resistance change, *i.e.*, the resistance of the junction with P alignment of the magnetic electrodes is higher than for AP alignment. The negative sign of the resistance change in CrO_2/Co MTJs has been attributed to the tunneling being dominated by negatively polarized *d*-like electrons due to predominantly $sd\sigma$ bonding at the interface [6–8].

In order to better control the spin orientation during the tunneling process and thereby enhance the TMR, we have developed a chemical vapor deposition (CVD) technique for heteroepitaxial growth of CrO_2/SnO_2 thin films on (100)-oriented TiO_2 substrates, with all of them possessing the rutile structure. With epitaxial SnO_2 as the barrier layer and polycrystalline Co as a counter-electrode, a positive TMR as high as 14% has been observed in the junctions at 5 K [8]. High-resolution STEM cross-sectional Z-contrast images of CrO_2/SnO_2 heterostructures indicate that the typical Cr_2O_3 layer, which is naturally formed on the CrO_2 surface, is absent after SnO_2 deposition. This is possibly because of its transformation to the rutile structure during growth of the SnO_2 layer [8]. A similar behavior has been observed for CrO_2/RuO_2 structures, where RuO_2 deposition eliminates the natural barrier on as-deposited CrO_2 films [4]. In this letter, we report on the observation of an anomalous bias dependence in CrO_2/SnO_2/Co MTJs as a function of the SnO_2 barrier thickness. A dramatic change in the magnetotransport

(a) Current address: Francis Bitter Magnet Laboratory, MIT - Cambridge MA 02139, USA; E-mail: gxmiao@mit.edu

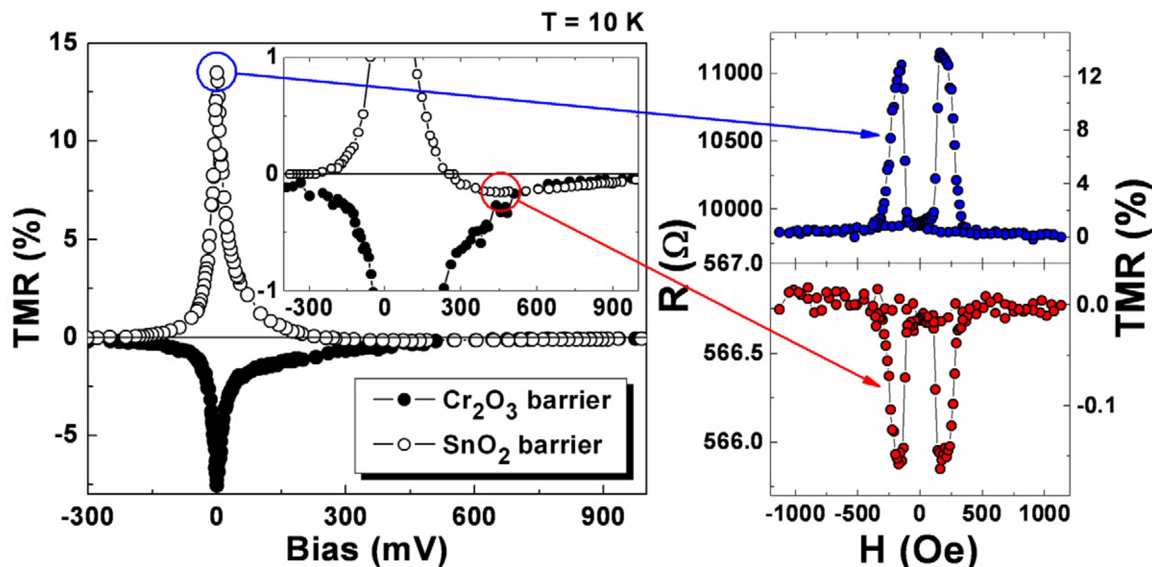

Fig. 1: (Colour on-line) Bias dependence for MTJs with 1.7 nm epitaxial SnO_2 barrier (open circles) and with Cr_2O_3 natural barrier (closed circles), with each data point derived from a corresponding MR loop. Typical TMR loops are illustrated on the right side. $T = 10\,K$.

characteristics from resonant TMR reversal behavior to a divergence of TMR at zero bias occurs in going from the ballistic (thin barrier) to the diffusive (thick barrier) transport regime. The latter corresponds to an electromotive force being generated on switching the relative magnetic moments of the CrO_2 and Co electrodes in the MTJ from P to AP alignment.

We deposited the epitaxial CrO_2/SnO_2 heterostructures by CVD on single crystal (100)-oriented TiO_2 substrates. Prior to loading into the furnace, the TiO_2 substrates ($5 \times 5\,mm^2$) were cleaned with organic solvents and dilute HF solution. The CrO_2 and SnO_2 layers were grown sequentially using CrO_3 and SnI_4 as precursors, respectively, with pure oxygen as the carrier gas. For optimal growth of the heteroepitaxial structures, the substrate temperature was maintained at 400 °C and 350 °C during the growth of the CrO_2 and SnO_2 layers, respectively. The top Co electrode was then deposited at room temperature in a separate chamber by magnetron sputtering. For the present study, the thicknesses of the bottom CrO_2 (100 nm) and top Co (50 nm) electrodes were kept fixed, while the SnO_2 barrier layer thickness was systematically varied. Standard optical lithography was used to fabricate MTJs using the trilayer structures with a junction area of $15 \times 3\,\mu m^2$. DC conductance was measured using the standard four-terminal method, while the AC conductance was determined by adding a small AC voltage modulation (∼1 mV, 80 Hz) to the junction and simultaneously recording dV across the junctions and dI across a series resistor. The second derivative, d^2I/dV^2, was then mathematically obtained by differentiating the dI/dV conductance curve. In the following, we define the polarity of the bias voltage with respect to the top Co electrode.

We begin by describing the transport properties of junctions when the SnO_2 barrier is sufficiently thin such that the transport is predominantly ballistic. An asymmetric bias dependence of the TMR is seen in fig. 1 for a MTJ with 1.7 nm thick barrier. The junction exhibits a rapid TMR drop with applied bias voltage, which is suggestive of the presence of spin flipping scattering centers both *inside the barrier* and *across the interfaces* [9]. Impurities are considered responsible for scattering inside the barrier, with the two primary scattering sources being Cr ions and oxygen vacancies. The former results from possible atomic-scale intermixing/diffusion at the SnO_2/CrO_2 interface, while the latter is known to occur naturally in SnO_2 —resulting in its semiconducting properties— as has also been theoretically confirmed from band structure calculations [10]. A consequence of the existence of impurity levels within the barrier is the occurrence of resonant TMR reversal with applied bias voltage, as seen in fig. 1, that can be attributed to the existence of impurity states within the barrier [11–13]. Depending on the barrier thickness, the TMR reversal occurs at a different bias voltage (between 250 and 400 mV DC). A natural generalization of the resonant tunneling model proposed by Tsymbal *et al.* [12] is that if the impurity energy levels are not pinned to one of the electrodes, *i.e.*, they are permitted to float with the applied bias due to the distribution of electrostatic potentials, then a TMR reversal will occur when the applied bias voltage exceeds a specific threshold in the negative-bias regime. Indeed, we have observed TMR reversals for both positive- and negative-bias voltages utilizing the AC measurement method (fig. 2), even though only one reversal at much higher bias is observed using the DC method. This can be understood

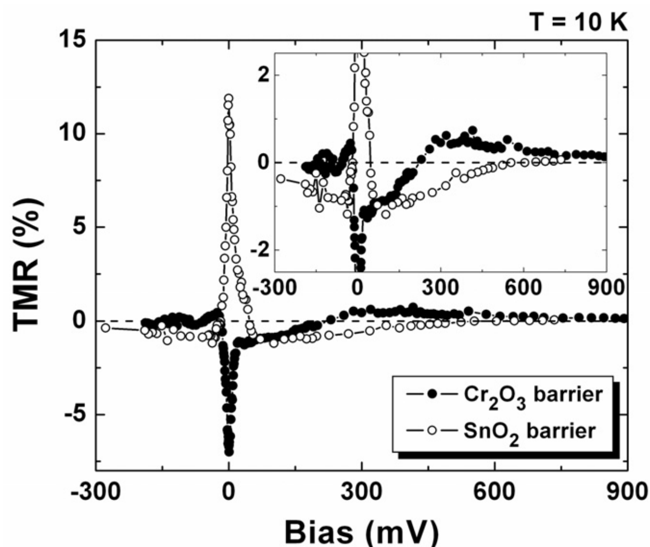

Fig. 2: Bias dependence of the AC TMR for a MTJ with 1.7 nm epitaxial SnO_2 barrier (open circles), and with Cr_2O_3 natural barrier (closed circles), with each data point derived from a corresponding MR loop. Inset shows the enlarged low TMR region. $T = 10$ K.

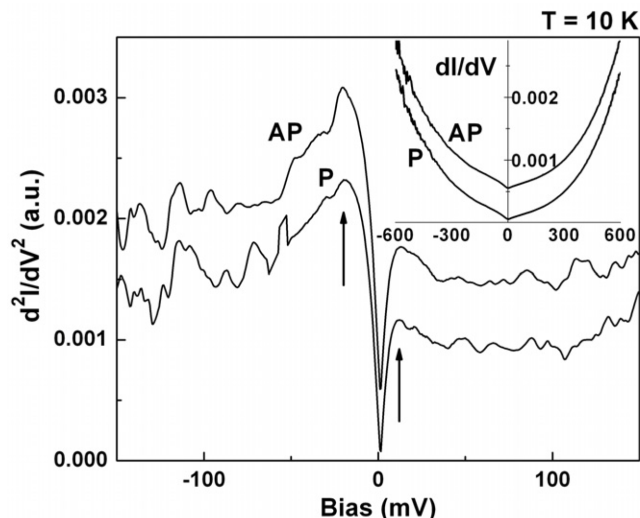

Fig. 3: IETS of the MTJ with 1.7 nm epitaxial SnO_2 barrier (arrows mark the magnon excitation positions) for AP and P alignments, with the curves derived from the corresponding conductance *vs.* V measurement as shown in the inset. In the inset, the curve for AP alignment is shifted upwards by one division for clarity.

based on the fact that the dynamic AC measurement probes the conductance *at the Fermi level* while the DC measurement accounts for the cumulative conductance *below the Fermi level*. The different reversal voltages in the positive- and negative-bias range results from the asymmetric positioning of the impurity levels inside the barrier.

The primary source of spin flipping at the interfaces is from magnon excitations. Magnons are collective spin wave excitations, and high-energy electrons can relax to the Fermi level by emitting a magnon that carries away the excess energy. Magnon excitations can be readily inferred from inelastic tunneling spectrum (IETS) measurements, for example, as demonstrated in Al_2O_3 and MgO-based MTJs [14–16]. Figure 3 shows the magnon excitations in the forward and reverse bias regimes. Because of the half-metallic nature of CrO_2, spin flipping processes are largely forbidden in the bulk, and magnon excitation is thus far weaker than in the counterpart ferromagnetic Co electrode of the tunnel junction. Clear asymmetry in the magnon strength can be observed in fig. 3. Since magnons have spin 1, the magnon-assisted tunneling process also leads to spin flipping and is thus detrimental to the TMR effect. The TMR decays much faster in the negative-biased as compared to the positive-biased branch, which is yet another signature that the magnon spectra differ dramatically in the CrO_2 and Co electrodes. If CrO_2 is fully half-metallic as predicted, the one-magnon process is expected to be completely suppressed and the only available route will be higher-order two-magnon processes [17]. This should result in more pronounced differences in the spectra as compared to the Co electrode. However, we expect the system to be further complicated by the existence of additional spin states, for example Cr^{3+} and Co^{2+}, at the interfaces which provide additional spin flipping sites that contribute to TMR reduction.

Next we examine the bias dependence in MTJs with thicker barriers that clearly exhibit a diffusive characteristic. The semiconducting properties of the barrier and the half-metallic nature of the electrode combine to yield a unique bias dependence for the system. Figure 4 shows the bias dependence of a junction with 4 nm thick SnO_2 barrier. The MR diverges at low bias and —within the detection limit of the system— *essentially approaches infinity close to zero bias.* The much more pronounced asymmetry in the conductance curve (fig. 4, inset) indicates the existence of charge transfer between the metal and the semiconductor layer, although the formation of an actual Schottky barrier is considered unlikely for a layer that is only 4 nm thick. Such a diverging MR behavior likely originates from a spin-dependent voltage shift across the semiconducting barrier. Figure 5 shows the voltage measured across the junction with sweeping an external magnetic field, but with no net flow of current (achieved by directly connecting the junction to a high-impedance nanovoltmeter). Two clearly distinguishable voltage states are observed, corresponding to the P and AP spin configurations. With varying SnO_2 thickness, the MTJ resistance displays a striking deviation from exponential dependence above 2 nm (fig. 5, inset), which indicates that the nature of charge transport changes from being mostly single step tunneling (ballistic) to multistep hopping (diffusive) with increasing barrier thickness. For each barrier thickness, we have checked a number of junctions with areas covering a range from $5 \times 1\,\mu\mathrm{m}^2$ up to $140 \times 28\,\mu\mathrm{m}^2$, and the voltage shift is found to be independent of the junction area as

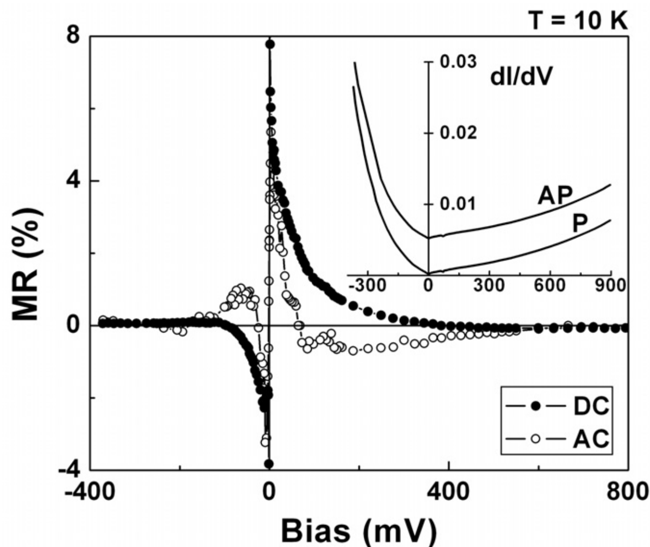

Fig. 4: DC (closed circles) and AC (open circles) bias dependence of a $CrO_2/SnO_2/Co$ MTJ with 4 nm SnO_2, with each data point derived from a corresponding MR loop. Inset shows the AC conductance dI/dV *vs.* bias voltage for AP and P alignments. In the inset, the curve for AP alignment is shifted upwards by one division for clarity.

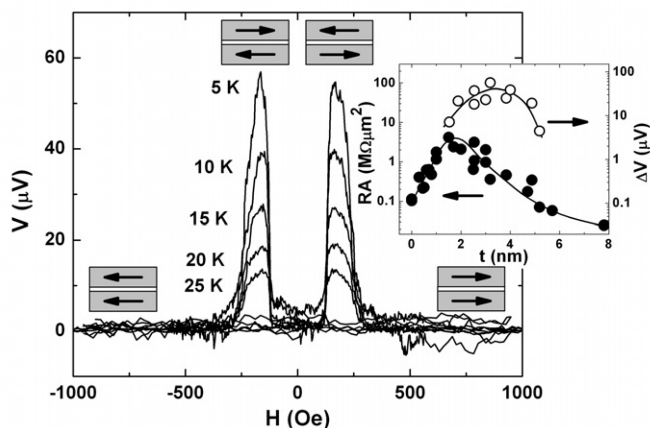

Fig. 5: Spin-dependent voltage shift with the application of an external field, for a MTJ with SnO_2 barrier thickness of 4 nm. Inset shows the variations of RA and ΔV as a function of barrier thickness at 10 K. The solid lines are provided only as a visual guide.

well as the junction impedance. On the other hand, the observed voltage shift is strongly dependent on the SnO_2 barrier thickness (fig. 5, inset).

In order to rule out possible complications from our processing and measurement setup, we performed a similar measurement on (CoFeB/MgO/CoFeB)-based MTJs, with the junction impedance chosen to closely match the previously described MTJs, and the junction TMR ($\sim$ 200% at 10 K) to be much larger. The MgO-based MTJs are patterned using the same lithographic process and tools, and measured with the same cryostat/electronics at the same temperature. Such a control experiment is designed to eliminate the possibility of voltage shift caused by electronic devices and/or grounding: if these are the cause, the MgO junctions should yield much higher-voltage responses with the sweeping of magnetic field. As expected, no spin-dependent voltage shift (within the noise level) has been observed in the MgO samples, which assures that the effect is not directly related to the TMR effect or measurement artifacts. To further rule out possible artifacts arising from contact voltages in the DC measurement setup, we have performed AC measurements on our samples, and the diverging nature of MR is again well captured as shown in fig. 4. Due to the modulation broadening of the signal, the AC MR does not actually approach infinity as in the case of DC MR, instead, a very sharp step-like turnover occurs in the zero bias region. The MR reversal can again be seen at slightly higher biases.

Our results provide strong evidence that besides quantum tunneling, there are other mechanisms cross linking the electrons' spin and charge degrees of freedom, leading to the observed spin-dependent voltage shift across the barrier. We hereby attempt to identify the possible origin of the observed effect. Firstly, this effect is established at equilibrium, therefore conventional active spin pumping mechanisms, such as spin battery or spin injection [18–20], are considered unlikely to be the cause of the observed phenomena. Secondly, the observed effect varies dramatically with temperature. A closely related phenomenon is the giant magneto-thermoelectric power [21] predicted in MTJ structures with magnon-assisted transport process. In FM/I/FM systems, the thermoelectric coefficient becomes spin dependent, and the difference between P and AP configurations can be as large as $55\,\mu V/K$ when half-metallic electrodes are used [21]. However, similar to other thermally activated processes, the magnon assisted process is predicted to actually increase with temperature. In addition, even though the temperature across the junction may be nonuniform, it is difficult to envision a temperature drop of 1 K across a barrier as thin as a few nm. Another possible cause of the observed phenomenon is some sort of magnetoelectric effect in the barrier layer, or at the interfaces [22]. While SnO_2 is not known to exhibit a magnetoelectric behavior, Cr_2O_3 is one of the first materials that was theoretically predicted [23] and experimentally confirmed [24] to be magnetoelectric, with its internal dipolar electric field directly coupled to its magnetic orientation. Though a nonvolatile voltage shift can in principle be generated this way, with possible Cr_2O_3 present at the CrO_2/SnO_2 interface, the expected magnitude is very small even with a perfect Cr_2O_3 layer.

We are presently unable to conclusively identify the origin of the observed spin-dependent voltage shift. An important concept of "spin battery" in MTJ structures was theoretically proposed [25] and experimentally demonstrated recently [26]. Although our device was not intentionally designed for this purpose, we believe

that the observation of an electromotive force induced by a static magnetic field in magnetic tunnel junctions containing MnAs quantum nanomagnets [26] is related to the spin-dependent voltage shift we observe in CrO_2-based MTJs. However, there is a significant difference in our experimental observation. The voltage shift persists in zero applied field, with two clear remnant states achievable when the FM layers are aligned in the P and AP states. In the absence of field-induced Zeeman energy, we need to identify other source(s) of spin energy accessible in our system.

Since the phenomenon appears to be related to the diffusive character of transport, we speculate that the underlying mechanism for the phenomenon may be analogous to that leading to Schottky barrier formation between a metal and a semiconductor. On the side of the half-metal, any spins diffusing across the barrier will be immediately flipped in the strong exchange field unless they are of the correct orientation. We speculate that the spin energy likely originates from the intrinsic exchange field, which has a large energy reservoir. We do not observe any significant decay in the induced voltage over a typical time scale of 30 minutes, with both open-circuit and closed-circuit (with a $10\,k\Omega$ resistor in series) configurations. The released exchange energy is normally carried away by magnons, yet this energy dissipation channel is virtually forbidden in half-metals. The spin conversion is thus constrained to appear in the form of an electromotive force. For example, it has been theoretically predicted that the conversion of a spin current from a half-metal to an unpolarized current in a normal metal indeed introduces an electrochemical potential difference between spin-up and spin-down electrons [27]. This suggests that higher temperatures will be detrimental to the observed phenomenon because of the introduction of additional spin flipping channels, as is indeed observed. In addition, a diffusive media is necessary for transport. In perfect tunnel barriers (such as in our MgO-based control junctions), no spin imbalance is possible due to the absence of available states. On the other hand, in fully metallic systems, the chemical potential shift due to spin diffusion [28–30] can be observed using the nonlocal detection geometry, and the spin signal ($\sim P^2/\sigma$) naturally increases by combining a half-metal (high spin polarization P) and semiconductor (low conductivity σ). Since the process relies on natural spin diffusion, the two ferromagnetic electrodes have to be placed very close to each other (∼nm) in such a nonlocal geometry in order for the spin analyzer to be coupled to the spin source.

In summary, we have studied the bias dependence in MTJs based on half-metallic CrO_2 electrode and epitaxial SnO_2 barrier layer. With thin barriers, impurity-mediated resonant tunneling gives rise to TMR reversals at certain bias voltages; while with thicker barriers, the diffusive nature of the transport results in a spin-dependent electromotive force, which is manifested as a diverging MR at zero bias.

***

We thank W. Butler and P. LeClair for useful discussions and suggestions. This research was supported by NSF MRSEC Grant No. DMR-0213985. GXM acknowledges support in part by the NSF under Grant No. DMR-0605966 and by the JHU MRSEC (NSF DMR-0520491).

REFERENCES

[1] Jullière M., *Phys. Lett. A*, **54** (1975) 225.
[2] Anguelouch A., Gupta A., Xiao G., Abraham D. W., Ji Y., Ingvarsson S. and Chien C. L., *Phys. Rev. B*, **64** (2001) 180408(R).
[3] Bratkovsky A. M., *Appl. Phys. Lett.*, **72** (1998) 2334.
[4] Miao G. X., Sims H., Gupta A., Butler W. H. and Ghosh S., *J. Appl. Phys.*, **97** (2005) 10C924.
[5] Gupta A., Li X. W. and Xiao G., *Appl. Phys. Lett.*, **78** (2001) 1894.
[6] Hertz J. A. and Aoi K., *Phys. Rev. B*, **8** (1973) 3252.
[7] Tsymbal E. Y. and Pettifor D. G., *J. Phys.: Condens. Matter*, **9** (1997) L411.
[8] Miao G. X., LeClair P., Gupta A., Xiao G., Varela M. and Pennycook S., *Appl. Phys. Lett.*, **89** (2007) 022511.
[9] Moodera J. S., Nassar J. and Mathon G., *Annu. Rev. Mater. Sci.*, **29** (1999) 381.
[10] Kilic C. and Zunger A., *Phys. Rev. Lett.*, **88** (2002) 095501 and references therein.
[11] Tsymbal E. Y. and Pettifor D. G., *Phys. Rev. B*, **64** (2001) 212401.
[12] Tsymbal E. Y., Sokolov A., Sabirianov I. F. and Doudin B., *Phys. Rev. Lett.*, **90** (2003) 186602.
[13] Sheng L., Xing D. Y. and Sheng D. N., *Phys. Rev. B*, **69** (2004) 132414.
[14] Dimopoulos T., Gieres G., Wecker J., Luo Y. and Samwer K., *Europhys. Lett.*, **68** (2004) 706.
[15] Ando Y., Miyakoshi T., Oogane M., Miyazaki T., Kubota H., Ando K. and Yuasa S., *Appl. Phys. Lett.*, **87** (2005) 142502.
[16] Miao G. X., Chetry K., Gupta A., Butler W. H., Tsunekawa K., Djayaprawira D. and Xiao G., *J. Appl. Phys.*, **99** (2006) 08T305.
[17] Miao G. X., Gupta A., Xiao G. and Anguelouch A., *Thin Solid Films*, **478** (2005) 159.
[18] Das Sarma S., Fabian J., Hu X. D. and Zutic I., *Solid State Commun.*, **119** (2001) 207.
[19] Schmidt G., *J. Phys. D: Appl. Phys.*, **38** (2005) R107.
[20] Hofmann M. R. and Oestreich M., in *Magnetic Heterostructures,* in *Springer Tracts Mod. Phys.*, **227** (2008) 335.
[21] McCann E. and Fal'ko V. I., *Phys. Rev. B*, **66** (2002) 134424.
[22] Rondinelli J. M., Stengel M. and Spaldin N. A., *Nat. Nanotechnol.*, **3** (2008) 46; Niranjan M. K., Velev J. P., Duan C.-G., Jaswal S. S. and Tsymbal E. Y., *Phys. Rev. B*, **78** (2008) 104405.

[23] Dzyaloshinskii I. E., *Sov. Phys. JEPT*, **37** (1960) 628.
[24] Astrov D. N., *Sov. Phys. JETP*, **11** (1960) 708; Rado G. T. and Folen V. J., *Phys. Rev. Lett.*, **7** (1961) 310.
[25] Barnes S. E. and Maekawa S., *Phys. Rev. Lett.*, **98** (2007) 246601.
[26] Hai P. N., Shinobu O., Masaaki T., Barnes S. E. and Maekawa S., *Nature*, **458** (2009) 489.
[27] van Son P. C., van Kempen H. and Wyder P., *Phys. Rev. Lett.*, **58** (1987) 2271.
[28] Johnson M. and Silsbee R. H., *Phys. Rev. Lett.*, **55** (1985) 1790.
[29] Valet T. and Fert A., *Phys. Rev. B*, **48** (1993) 7099.
[30] Jedema F. J., Heersche H. B., Filip A. T., Baselmans J. J. A. and van Wees B. J., *Nature*, **416** (2002) 713.